Quantitation of the Anomeric Effect in Adenosine and Guanosine by Comparison of the Thermodynamics of the Pseudorotational Equilibrium of the Pentofuranose Moiety in *N*- and *C*-Nucleosides

Christophe Thibaudeau, Janez Plavec, and Jyoti Chattopadhyaya*

Contribution from the Department of Bioorganic Chemistry, Box 581, Biomedical Centre, University of Uppsala, S-751 23 Uppsala, Sweden

Received April 20, 1994®

Abstract: The effect of *N*-aglycones at C1′ on the drive of two-state north (N (C3′-*endo*-C2′-*exo*)) ⇄ south (S (C2′-*endo*-C3′-*exo*)) pseudorotational equilibrium in β-D-ribofuranosyl-*N*-nucleosides consists of two counteracting contributions from (i) the anomeric effect (stereoelectronic interactions between furanose O4′ and the nucleobase nitrogen at C1′), which places the aglycone in the pseudoaxial orientation, and (ii) the inherent steric effect of the nucleobase, which opposes the anomeric effect by its tendency to take up pseudoequatorial orientation. The maximum pseudoequatorial orientation of the nucleobase is sterically possible only in the S-type conformations. Therefore, the extent of this pseudoequatorial orientation can be experimentally determined by the extent of the thermodynamic stabilization of the S conformer in the two-state N ⇄ S equilibrium (ref 1). This means that a direct measurement of the extent of thermodynamic stabilization of the S conformer amongst a set of various β-D-ribofuranosyl-*C*-nucleosides, where the absence of the anomeric effect has been previously established from X-ray studies (ref 6), should give us a reference point for the maximally pseudoequatorially oriented *C*-nucleobase. We report here the characterization of this reference β-D-ribofuranosyl-*C*-nucleoside. The subtraction of the $\Delta H°$ of its pseudorotational equilibrium from the $\Delta H°$ of β-D-ribofuranosyl-*N*-nucleosides gave the quantitative insight of the anomeric effect in adenosine (+9.1 kJ/mol) and guanosine (+10.5 kJ/mol) for the first time. We have found that the *C*-aglycones in formycin A (**1**) and B (**2**) constitute the optimal reference point (ref 12) for our purpose because they take up the predominantly favored pseudoequatorial orientation (closer to the limit), where the steric control is almost the exclusive determinant, owing to the negligible presence of any stereoelectronic interaction with the lone pairs of furanose-O4′ (see Table 3).

Introduction

The drive of the two-state N ⇄ S pseudorotational equilibrium of the sugar moiety of β-D-ribofuranosyl-*N*-nucleosides in solution is energetically controlled by various stereoelectronic gauche and anomeric effects.[1-3] The gauche effects[4] of O4′—C4′—C3′—O3′ and O2′—C2′—C1′—N fragments drive the sugar pseudorotational equilibrium toward S,[1a] whereas it is driven to N by the gauche effect of O4′—C1′—C2′—O2′ (Scheme 1).

The X-ray crystal structures of *N*-nucleosides show the shortening[3] of the O4′—C1′ bond relative to C4′—O4′ by about 0.03 Å, which has been considered as a manifestation of the anomeric effect. The origin of the anomeric effect has been previously attributed to the following: (i) favorable n → σ* molecular orbital overlap which favors pseudoaxial orientation of the *N*-substituent, (ii) destabilization of the pseudoequatorial conformer in order to achieve minimal dipole–dipole electrostatic interaction, or (iii) a hyperconjugative effect.[5] In β-D-ribofuranosyl-*C*-nucleosides, however,[6] the difference between O4′—C1′ and O4′—C4′ bond lengths is much smaller (≈0.01 Å) compared to β-D-ribofuranosyl-*N*-nucleosides (≈0.03 Å), which suggests that the aglycone in the former does not induce any anomeric effect. On the basis of a regressional analysis performed in a parallel study[1,7a] on a set of $\Delta H°$ values for the N ⇄ S pseudorotational equilibrium of (*S*)-tetrahydrofurfuryl alcohol, 1-deoxy-D-ribofuranose, 1,2-dideoxy-D-ribofuranose, and 2′,3′-dideoxy-β-D-ribofuranosyl-, 2′-deoxy-β-D-ribofuranosyl-, and β-D-ribofuranosylpurine and -pyrimidine derivatives, we derived the $\Delta H°$ contribution for the sum of the intractable anomeric and steric effects in adenosine, guanosine, and cytidine[1,7a] and also the gauche effect involving O2′ and anomeric nitrogen (*i.e.* O2′—C2′—C1′—N(purine)).[7a] A qualitative comparison of the $\Delta H°$ values[1,7a] for the *N*-substituent effect, however, clearly showed that the larger $\Delta H°$ value for cytidine compared to

Scheme 1. Dynamic Two-State Equilibrium of N ⇄ S Pseudorotamers of β-d-Ribofuranosyl-*C*-nucleosides in Solution

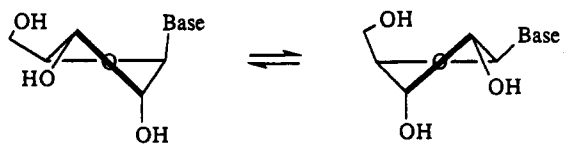

North sugar (C_3-*endo*-C_2-*exo*) South sugar (C_2-*endo*-C_3-*exo*)

• Abstract published in *Advance ACS Abstracts,* August 1, 1994.

(1) (a) Plavec, J.; Tong, W.; Chattopadhyaya, J. *J. Am. Chem. Soc.* **1993**, *115*, 9734. (b) Plavec, J.; Garg, N.; Chattopadhyaya, J. *J. Chem. Soc., Chem. Commun.* **1993**, 1011. (c) Plavec, J.; Koole, L. H.; Chattopadhyaya, J. *J. Biochem. Biophys. Methods* **1992**, *25*, 253. (d) For a preliminary communication on the structures of pyrimidine *C*-nucleosides, see: Thibaudeau, C.; Plavec, J.; Watanabe, K. A.; Chattopadhyaya, J. *J. Chem. Soc., Chem. Commun.* **1994**, 537. (e) Thibaudeau, C.; Plavec, J.; Garg, N.; Papchikhin, A.; Chattopadhyaya, J. *J. Am. Chem. Soc.* **1994**, *116*, 4038. (f) Plavec, J.; Thibaudeau, C.; Viswanadham, G.; Sund, C.; Chattopadhyaya, J. *J. Chem. Soc., Chem. Commun.* **1994**, 781. (g) Koole, L. H.; Buck, H. M.; Nyilas, A.; Chattopadhyaya, J. *Can. J. Chem.* **1987**, *65*, 2089. (h) Koole, L. H.; Buck, H. M.; Bazin, H.; Chattopadhyaya, J. *Tetrahedron* **1987**, *43*, 2289. (i) Plavec, J.; Thibaudeau, C.; Chattopadhyaya, J. *J. Am. Chem. Soc.* **1994**, *116*, 6558–6560.

(2) Altona, C.; Sundaralingam, M. *J. Am. Chem. Soc.* **1972**, *94*, 8205. *Ibid.* **1973**, *95*, 2333.

(3) Saenger, W. *Principles of Nucleic Acid Structure*; Springer-Verlag: Berlin, 1988.

(4) (a) Olson, W. K.; Sussman, J. L. *J. Am. Chem. Soc.* **1982**, *104*, 270. (b) Olson, W. K. *J. Am. Chem. Soc.* **1982**, *104*, 278.

(5) (a) Perrin, C. L.; Armstrong, K. B.; Fabian, M. A. *J. Am. Chem. Soc.* **1994**, *116*, 715. (b) Ellervik, U.; Magnusson, G. *J. Am. Chem. Soc.* **1994**, *116*, 2340.

0002-7863/94/1516-8033$04.50/0 © 1994 American Chemical Society

guanosine and adenosine is owing to the tendency of bulky purine aglycones to oppose the anomeric effect more effectively by being more pseudoequatorial than cytosine.

The gauche effects of O4′—C4′—C3′—O3′ and O4′—C1′—C2′—O2′ fragments and the effect of the 4′-CH_2-OH group are a constant factor in both β-D-ribofuranosyl-*N*- and -*C*-nucleosides, while the strengths of the gauche effect of the O2′—C2′—C1′—N-substituent in *N*-nucleosides or the steric and stereoelectronic effects of the aglycone in 8-aza-9-deaza-adenosine (formycin A, **1**), 8-aza-9-deazainosine (formycin B, **2**), 9-deazaadenosine (**3**), tiazofurin (**4**), Ψ-isocytidine (**5**),[1d] Ψ-isocytidine hydrochloride (**6**),[1d] 1-methyl-Ψ-uridine (**7**),[1d] 1,3-dimethyl-Ψ-uridine (**8**),[1d] and β-D-ribofuranosyl-*N*-nucleosides[1a,7] on the drive of N ⇄ S pseudorotational equilibrium of the constituent sugar depend upon the chemical nature of purine or pyrimidine[1d] heterocycles at C1′ compared to the reference compound 1-deoxy-D-ribofuranose **9**.[1a]

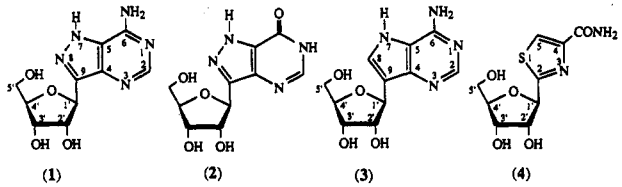

(1) (2) (3) (4)

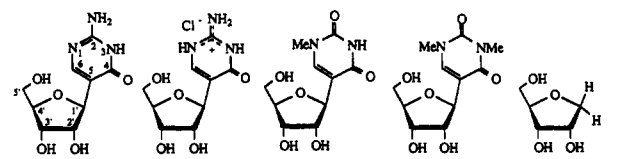

(5) (6) (7) (8) (9)

We have earlier shown[1d] through a comparison of the $\Delta H°$ values of the pseudorotational equilibria in **5**–**8** that the substituent effect of the pyrimidine base as the *C*-aglycone mainly operates by the through-space interaction between the conjugated 5,6-en-4-one and lone pairs of O4′ or O2′ and that the extent of the delocalization of the 5,6-en-4-one system and its interaction with O4′ lone pairs actually dictates the bias of the N ⇄ S pseudorotational equilibrium.[1d] We herein report that only the aromatic systems of purine aglycones such as pyrazolo[4,3-*d*]-pyrimidines in formycin A (**1**) and B (**2**),[8] amongst all other β-D-ribofuranosyl-*C*-nucleosides **1**–**8**, almost insignificantly interact with the lone pairs of furanose-O4′, which allow these purine aglycones to take up almost exclusively pure pseudoequatorial orientation owing to the minimization of the stereoelectronic interactions. This means that a simple subtraction of the $\Delta H°$ value of a purine β-D-ribofuranosyl-*N*-nucleoside from the sum of the average of $\Delta H°$ values of the N ⇄ S pseudorotational equilibria of purine β-D-ribofuranosyl-*C*-nucleosides **1** and **2** and the gauche effect of O2′—C2′—C1′—N(purine) should give us a direct measure of the energetic contribution of the O4′—C1′—N9 anomeric effect in adenosine and guanosine. (The sign of $\Delta H°$ is arbitrarily chosen[1] depending upon the natural log of the ratio of the population of S versus N conformers or vice versa. In our van't Hoff plots,[1] we have chosen the first alternative in the subsequent discussions. The positive $\Delta H°$ indicates the drive of N ⇄ S equilibrium to N, while the negative sign describes the drive to the S conformer.)

Table 1 shows the temperature-dependent $^3J_{HH}$ extracted from 1D ^{1}H-NMR spectra recorded at 500 MHz. The conformational hyperspace of the sugar pseudorotamers and the shift of the molar fractions of N (X_N) and S (X_S) conformers have been estimated from the experimental $^3J_{HH}$ coupling constants at different temperatures (Table 2); subsequently, the geometry of these conformers have been used to back-calculate $^3J_{HH}$ by the Karplus–Altona equation,[9c] and the errors have been assessed in terms of root mean square and the largest deviation between the experimental and calculated coupling constants (ΔJ_{max}) using the

Table 1. Vicinal $^3J_{H,H}$ Coupling Constants[a] and Distribution of the Rotamers around the $C_{4'}$—$C_{5'}$ Bond[b] for **1**–**4** at Two Extreme Temperatures

C-nucleoside	*T* (K)	$J_{1'2'}$	$J_{2'3'}$	$J_{3'4'}$	$J_{4'5'}$	$J_{4'5''}$	x (γ^+)	x (γ^t)	x (γ^-)
1[c,d]	278	7.8	5.2	3.0	2.8	3.5	0.73	0.23	0.04
	358	6.9	5.5	4.1	3.2	4.3	0.61	0.30	0.09
2[c,e]	278	7.7	5.3	3.2	2.9	3.7	0.70	0.25	0.05
	358	6.8	5.5	4.2	3.4	4.5	0.57	0.32	0.11
3[c,f]	278	7.6	5.3	2.6	3.0	3.0	0.76	0.17	0.07
	363	7.2	5.6	3.7	3.3	4.0	0.63	0.27	0.10
4[c,g]	278	5.4	4.9	5.1	3.1	5.4	0.50	0.43	0.07
	358	5.5	5.3	5.0	3.7	5.6	0.42	0.43	0.15

[a] $^3J_{H,H}$ (in Hz, error ±0.1 Hz) were extracted from 1D 500-MHz ^{1}H-NMR spectra recorded in D_2O solution in 10 K steps between 278 and 358 K for **1**, **2**, and **4**, between 278 and 363 K for **3**. All spectra were simulated using the DAISY program.[10] [b] The populations of the γ-rotamers across the C4′—C5′ bond were calculated following the procedure of Haasnoot *et al.* (*Recl. Trav. Chim. Pays-Bas* **1979**, *98*, 576). [c] Negligible changes in the chemical shift (<0.05 ppm) of all protons over the whole temperature range (278–358 K) suggest the absence of aggregation at 20 mM concentration for **1**–**4**. [d] δ (298 K, MeCN ≡ 2.00 ppm) 8.30 (H-2), 5.32 (H-1′), 4.71 (H-2′), 4.45 (H-3′), 4.32 (H-4′), 4.01 (H-5′), 3.89 (H-5″) ppm. [e] δ (298 K) 8.12 (H-2), 5.30 (H-1′), 4.66 (H-2′), 4.43 (H-3′), 4.30 (H-4′), 3.99 (H-5′), 3.88 (H-5″) ppm. [f] δ (298 K) 8.34 (H-8), 7.75 (H-2), 4.99 (H-1′), 4.24 (H-2′), 4.23 (H-3′), 4.12 (H-4′), 3.83 (H-5′), 3.82 (H-5″) ppm. [g] δ (298 K) 8.35 (H-5), 5.27 (H-1′), 4.45 (H-2′), 4.29 (H-3′), 4.27 (H-4′), 3.96 (H-5′), 3.87 (H-5″) ppm.

(6) (a) The differences between C4′—O4′ and O4′—C1′ bond distances in X-ray crystal structures of most β-D-ribofuranosyl-*C*-nucleosides are smaller (≈0.01 Å) than in *N*-counterparts (≈0.03 Å), and therefore we conclude that the anomeric effect is absent in β-D-ribofuranosyl-*C*-nucleosides. For the X-ray crystal structures of pyrimidine β-D-ribofuranosyl-*C*-nucleoside 4-thio-ψ-uridine, see: Barnes, C. L.; Hawkinson, S. W.; Wigles, P. W. *Acta Crystallogr., Sect. B* **1980**, *36*, 2299. For isocytidine hydrochloride, see: Birnbaum, G. I.; Watanabe, K. A.; Fox, J. J. *Can. J. Chem.* **1980**, *58*, 1633. For 2′-chloro-2′-deoxy-1,3-dimethyl-ψ-uridine, see: Pankiewicz, K. W.; Watanabe, K. A.; Takayanagi, H.; Itoh, T.; Ogura, H. *J. Heterocycl. Chem.* **1985**, *22*, 1703. The X-ray crystal structures of some purine β-D-ribofuranosyl-*C*-nucleosides have been also elucidated by the following: Koyama, G.; Nakamura, H.; Umezawa, H.; Iitaka, Y. *Acta Crystallogr., Sect. B* **1976**, *32*, 813 (for formycin B (**2**)). Abola, J. E.; Sims, M. J.; Abraham, D. J.; Lewis, A. F.; Townsend, L. B. *J. Med. Chem.* **1974**, *17*, 62 (for 2-methylformycin A). Prusiner, P.; Brennan, T.; Sundaralingam, M. *Biochemistry* **1973**, *12*, 1196 (for formycin A monohydrate). (b) From a X-ray study (Goldstein, B. M.; Takusagawa, F.; Berman, H. M.; Srivastava, P. C.; Robins, R. K. *J. Am. Chem. Soc.* **1983**, *105*, 7416) it has been found that tiazofurin (**4**) crystallizes with a S sugar pseudorotamer (P_S = 154.9°, Ψ_m = 43.4°) and that the conformation around its *C*-glycosyl bond is such that the thiazole-sulfur forms a close intramolecular contact with O4′. This latter finding has been interpreted in terms of an attractive intramolecular interaction in the thiazole nucleosides between the positively charged thiazole sulfur and the lone pairs of O4′, as confirmed by molecular orbital calculations. It has been also suggested that the intramolecular S···O4′ electrostatic contact would impose constraints on the *C*-glycosyl bond which may be required for an optimal activity of tiazofurin. Clearly, these stereoelectronic interactions in tiazofurin (**4**) result in the drive of its N ⇄ S pseudorotational equilibrium in solution toward N-type sugar conformations, giving a positive $\Delta H°$ value (Table 3).

(7) (a) In this unpublished work, $\Delta H°$ values have been recalculated using the PSEUROT[9] program (version 5.4 with the latest λ-electronegativity set (from July, 1992); see footnotes of Table 2). These new $\Delta H°$ values have been the basis for an updated regressional analysis using our methodology that is already described in ref 1a. In this new regression analysis we have also taken into consideration the $\Delta H°$ values for the pseudorotational equilibrium of thymidine, uridine, 3′-AMP, 2′-dAMP, 3′-ethylphosphate of 2′-dA,[1f] 3′-GMP, 2′-dGMP, 3′-ethylphosphate of 2′-dG,[1f] 3′-CMP, 2′-dCMP, 3′-ethylphosphate of 2′-dC,[1f] UMP, 2′-dUMP,[7b] TMP, and 3′-ethylphosphate of T[1f] in addition to the ones described[1a] (a total set of 30 compounds for the new extended version of the old regression analysis[1a]). As a result of this extended regression analysis, the standard deviations of the values of the stereoelectronic effects varied between 0.4 and 1.1 kJ/mol and are reduced compared to old standard deviations (1.3 ± 0.5) described in ref 1a. (b) Unpublished work.

(8) For the IUPAC nomenclature of these heterocycles see: Chenon, M.-T.; Panzica, R. P.; Smith, J. C.; Pugmire, R. J.; Grant, D. M.; Townsend, L. B. *J. Am. Chem. Soc.* **1976**, *98*, 4736.

(9) (a) de Leeuw, F. A. A. M.; Altona, C. *J. Comput. Chem.* **1983**, *4*, 438. (b) Donders, L. A.; de Leeuw, F. A. A. M.; Altona, C. *Magn. Reson. Chem.* **1989**, *27*, 556. (c) Altona, C.; Ippel, J. H.; Hoekzema, A. J. A. W.; Erkelens, C.; Groesbeek, G.; Donders, L. A. *Magn. Reson. Chem.* **1989**, *27*, 564.

(10) DAISY, Spin Simulation Program, was provided by Bruker.

(11) PROFIT II 4.1, Quantum Soft, Postfach 6613, CH-8023 Zürich, Switzerland, 1993.

Table 2. Hyperspace of Geometries of the N and S Sugar Pseudorotamers Assessed by the PSEUROT[9] Analyses of Vicinal $^3J_{H,H}$ of *C*-Nucleosides **1–4**

	PSEUROT fitting process[a]			
compds	(i) $\Psi_N = \Psi_S$ fixed	(ii) P_N and Ψ_N fixed	rms (Hz)	ΔJ_{max}[b] (Hz)
1	$[-42° < P_N < 11°] \rightleftarrows [126° < P_S < 138°]$	$127° < P_S < 144°$ with $32° < \Psi_S < 46°$	<0.2	<0.5
2	$[-42° < P_N < -8°] \rightleftarrows [125° < P_S < 134°]$	$126° < P_S < 141°$ with $32° < \Psi_S < 46°$	<0.2	<0.4
3	$[-48° < P_N < -17°] \rightleftarrows [128° < P_S < 138°]$	$132° < P_S < 146°$ with $30° < \Psi_S < 40°$	<0.2	<0.5
4	$[-30° < P_N < 33°] \rightleftarrows [120° < P_S < 148°]$		<0.2	<0.4

[a] The PSEUROT analyses (24 calculations for **1–3**, 11 for **4**) of the temperature-dependent $^3J_{HH}$ have been performed either (i) by fixing Ψ_m of both N and S pseudorotamers to an identical value in the range 37–45° for **1** and **2**, 35–43° for **3**, and 34–44° for **4** (1° resolution) or (ii) by constraining successively P_N of the minor N pseudorotamer to −36°, −18°, 0°, 18°, and 36° with Ψ_N set to 37°, 41°, and 45° for **1** and **2** and to 35°, 39°, and 43° for **3**. The following λ-electronegativities[9c] were used in the PSEUROT input files for the substituents on H—C—C—H fragments: O4′, 1.27; *C*-aglycone, 0.45; OH, 1.26; C1′, C2′, C3′, C4′ 0.62; and C5′, 0.68. [b] ΔJ_{max} is the largest deviation observed between experimental $^3J_{HH}$ and the coupling constants back-calculated using both PSEUROT fitting processes.

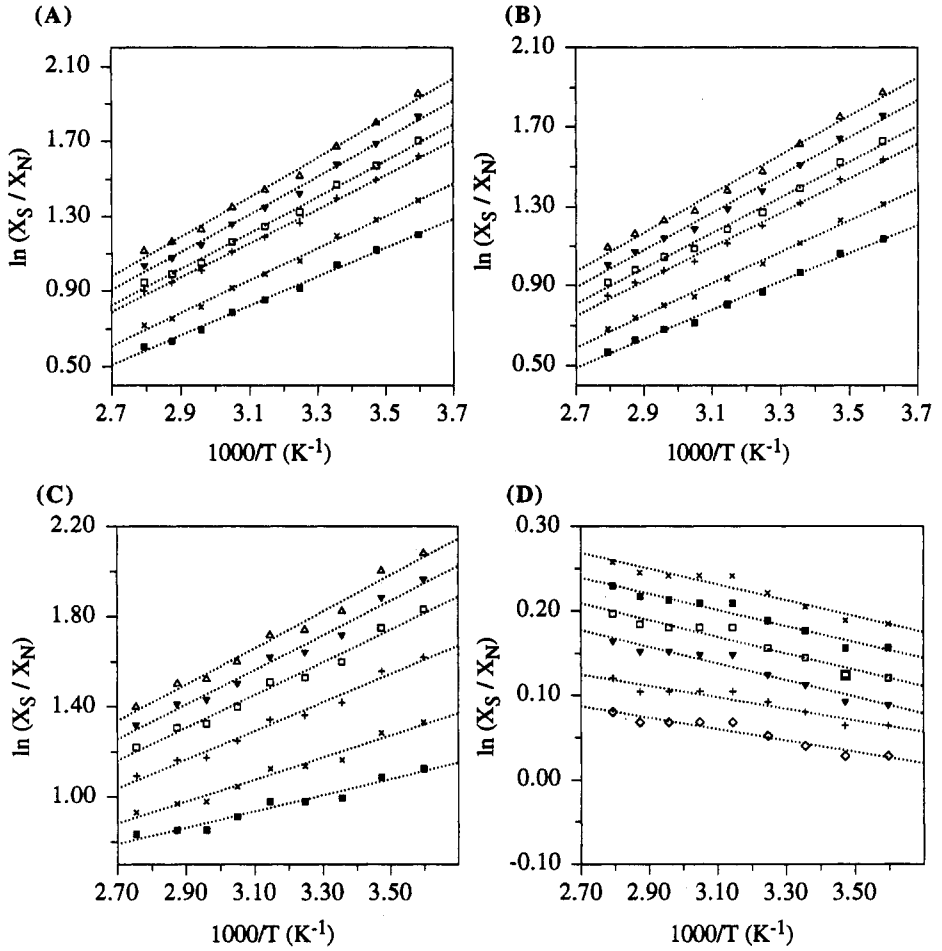

Figure 1. Van't Hoff plots of $\ln(X_S/X_N)$ as a function of $1000/T$ for **1** (A), **2** (B), **3** (C), and **4** (D). The natural logarithm of the mole fractions X_S and X_N from various PSEUROT[9] analyses of temperature-dependent $^3J_{HH}$ was used to perform least-squares fitting processes with PROFIT[11] to give as many straight lines as possible (see Table 2 for the conformational space covered by the PSEUROT[9] analyses). For clarity we only show representative plots based on the following PSEUROT[9] analyses: Ψ_m of both N and S conformers were constrained to 37° (+), 41° (×), and 45° (■) for **1** and **2**, to 35° (+), 39° (×), and 43° (■) for **3**, and to 36° (◇), 37° (+), 38° (×), 39° (■), 40° (□), and 41° (▼) for **4**. P_N was also set to 0° for **1** and **2** (Ψ_N = 37° (□), 41° (▼), 45° (△)) and **3** (Ψ_N = 35° (□), 39° (▼), and 43° (△)). Individual enthalpy ($\Delta H°$) and entropy ($\Delta S°$) values were derived from the slopes and intercepts, respectively, of each van't Hoff plot according to the relation $\ln(X_S/X_N) = -(\Delta H°/R)(1000/T) + \Delta S°/R$ and were used subsequently to calculate average $\Delta H°$ and $\Delta S°$ contributions to the N ⇄ S equilibrium of **1–4** (Table 3).

program PSEUROT[9] (see Table 2). Figure 1 shows the typical van't Hoff plots of the natural logarithm of the ratio of the populations of N and S conformers obtained from PSEUROT analyses, whereas Table 3 shows experimental enthalpy ($\Delta H°$) and entropy ($\Delta S°$) values of the two-state N ⇄ S pseudorotational equilibria of the sugar moieties of **1–4** and **5–8**[1d] (see Experimental Section for the details of the methodology). Note that we have only considered a two-state dynamic N ⇄ S pseudorotational equilibrium for the van't Hoff-type analysis since there is no experimental evidence (NMR) for a third state (see refs 15–17 in ref 1d and ref 17 in ref 1e) in the solution.

Results and Discussion

At 298 K, for the purine β-D-ribofuranosyl-*C*-nucleosides **1–3** and Ψ-isocytidine (**5**), the $\Delta H°$ contribution prevails over the counteracting $-T\Delta S°$ term and drives the N ⇄ S pseudorotational equilibrium to the S conformer (Table 3). On the other hand, the $\Delta H°$ contribution for the β-D-ribofuranosyl-*C*-nucleosides **4**, **7**, and **8** drives the sugar conformation to the N, and it is overridden at 298 K by the $-T\Delta S°$ term, which favors S-type pseudorotamers, as evident from the ca. 1:1 ratio of N and S conformers at the pseudorotational equilibrium. A particular heterocycle at C1′ in purine β-D-ribofuranosyl-*C*-nucleoside **3** or in thiazolo **4** and

Table 3. $\Delta H°$ and $\Delta S°$ of N ⇄ S Equilibrium in C-Nucleosides **1–8** and 1-Deoxy-D-ribofuranose (**9**)[a]

compds	$\Delta H°$ [b]	$\Delta S°$ [b]	$-T\Delta S°$ [b]	$\Delta\Delta H°$ [c]	ΔG^{298} [b]	$\%S^{278}$ [d]	$\%S^{358}$ [d]	$\Delta\%S$[e] (358–278 K)
1	−7.7 (0.7)	−14.7 (0.9)	4.4	−8.1	−3.3	83	69	−14
2	−7.1 (0.6)	−13.4 (0.8)	4.0	−7.5	−3.1	81	68	−13
3	−5.2 (1.2)	−5.4 (2.0)	1.6	−5.6	−3.6	83	75	−8
4	0.8 (0.1)	3.7 (1.2)	−1.1	0.4	−0.3	52	54	+2
5[f]	−2.1 (0.3)	−3.0 (2.0)	0.9	−2.5	−1.2	63	58	−5
6[f]	3.9 (0.2)	12.5 (0.6)	−3.7	3.5	0.2	45	55	+10
7[f]	0.9 (0.2)	5.1 (0.8)	−1.5	0.5	−0.6	55	58	+3
8[f]	2.0 (0.2)	7.9 (0.5)	−2.4	1.6	−0.4	52	57	+5
9	0.4 (1.1)	−5.1 (3.5)	1.5	0.0	1.9	31	32	+1

[a] Data taken from ref 7. [b] $\Delta H°$, $-T\Delta S°$ (at 298 K), and ΔG^{298} are given in kJ/mol, $\Delta S°$ in J/mol K. $\Delta H°$ and $\Delta S°$ (σ are indicated in parentheses) are average values derived from the slopes and intercepts, respectively, of a series of van't Hoff plots of $\ln(X_S/X_N)$ as a function of $1000/T$ based on the results of various PSEUROT[9] analyses (see Figure 1 for representative van't Hoff plots and Table 2 for the geometries of N and S pseudorotamers optimized with PSEUROT[9]). The positive and negative signs of $\Delta H°$ and $-T\Delta S°$ contributions indicate that the pseudorotational equilibrium is driven to the N or S conformers, respectively. [c] $\Delta\Delta H°$ (in column 5) = $\Delta H°$ (of **1–9** in column 2) − $\Delta H°$ (of **9** in column 2) represent the substituent effect of the C-aglycone in **1–8** compared to reference **9**. [d] At T K, $\%S(T) = 100[\exp(-\Delta G^T/RT)]/[\exp(-\Delta G^T/RT) + 1]$. [e] $\Delta\%S$ (358–278 K) = $\%S^{358} - \%S^{278}$ shows the change of population of south-type sugar owing to the net result of the $\Delta H°$ and $-T\Delta S°$ contribution as a function of temperature: for **1–3** and **5**, negative $\Delta H°$ values drive the N ⇄ S equilibrium to the S and are opposed by minor $-T\Delta S°$ terms which drive, however, more to the N at 358 K than at 278 K. Therefore, the population of the major S conformers decreases upon increase of the temperature from 278 to 358 K (negative $\Delta\%S$ (358–278 K)). For **4**, **7**, and **8** $\Delta H°$ drive to the N but are overridden by counteracting $-T\Delta S°$ terms which drive even more to the S at higher temperatures, which yields positive $\Delta\%S$ (358–278 K) values. Finally, for **6** the sign of $\Delta G°$ changes from positive at 278 K (at this temperature, positive $\Delta H°$ prevails over negative $-T\Delta S°$ and the sugar adopts preferentially the N conformation) to negative at 358 K (the pseudorotational equilibrium is then pushed to the S conformations owing to the major negative $-T\Delta S°$ contribution). [f] Data taken from ref 1d.

pyrimidine β-D-ribofuranosyl-*C*-nucleosides **5–8** influences the drive of the N ⇄ S pseudorotational equilibrium by combination of both steric and stereoelectronic effects,[1b,d] whereas the orientation of the purine heterocycle at C1′ in **1** and **2** is almost exclusively determined by the steric effect *(vide infra)*. The overall *C*-substituent effect of a specific aglycone can be assessed by simple subtraction of the $\Delta H°$ value for 1-deoxyribofuranose (**9**) from that of a β-D-ribofuranosyl-*C*-nucleoside **1–8**. (For $\Delta\Delta H°$ (*i.e.* *C*-substituent effect) values see column 5 in Table 3. The larger positive to larger negative $\Delta H°$ and $\Delta\Delta H°$ values in Table 3 suggest more N to more S sugar stabilization, respectively.) Since steric hindrance in a β-D-ribofuranosyl-*C*-nucleoside is reduced by placing its C1′-substituent in the pseudoequatorial orientation, which is achieved in S-type conformations, the more the S sugar pseudorotamer is stabilized, the larger the negative $\Delta\Delta H°$ value, and the larger the magnitude of the pseudoequatorial orientation of the C1′ substituent. A perusal of the data reported in Table 3 clearly shows that the purine aglycones in **1** and **2** are in purer pseudoequatorial orientation than in **3**. The order of the purity of sterically dictated pseudoequatorial orientation amongst thiazolo and pyrimidine β-D-ribofuranosyl-*C*-nucleosides is difficult to distinguish wholly on the basis of the steric bulk because in tiazofurin (**4**) a specific interaction involving thiazole-sulfur and furanose-O4′ is evident from its X-ray structure.[6b] It is, however, more straightforward to classify the *C*-aglycones in purine β-D-ribofuranosyl-*C*-nucleosides **1–3** and pyrimidine β-D-ribofuranosyl-*C*-nucleosides **5–8** on the basis of the extent of the pseudoequatorial orientation based on $\Delta\Delta H°$ values, as shown in Table 3: purine (**1** = **2** > **3**) ≫ pyrimidine (**5** > **7** > **8** > **6**). Within both groups, the steric contributions are, however, counteracted by the inherent stereoelectronic effect, which increases in the reverse order as the *C*-aglycone takes up the pseudoaxial orientation, which in turn pushes the N ⇄ S pseudorotational equilibrium to the more N-type sugar.

The negative sign and magnitude of the $\Delta H°$ values of the N ⇄ S equilibria in formycin A (**1**) and B (**2**) suggest that the interaction between the π-electron system involving the N^8—C^9 double bond and O4′, owing to the conjugation of the N^8—C^9 double bond with the conjugated fused π-deficient pyrimidine system, is minimal or is closer to the limit where the steric control is almost exclusively dominant, resulting in the maximal pseudoequatorial orientation of the *C*-aglycone.[12] The almost identical $\Delta H°$ values for formycin A (**1**) and B (**2**) show that π-electron clouds involving the N^8—C^9 double bonds are delocalized to a similar extent in both pyrazolo[4,3-*d*]pyrimidine moieties. *Thus, the nature of the pyrimidine part in the pyrazolo[4,3-d]-pyrimidine moieties in 1 and 2 has almost no specific and significant influence on the pseudoequatorial preference of the aglycone.* The comparison of $\Delta H°$ values in 9-deazaadenosine (**3**) with formycin A (**1**) or formycin B (**2**) also shows that the π-electrons of the C^8—C^9 double bond in the pyrrole moiety are less delocalized than those of N^8—C^9 in the pyrazole moiety and therefore more available for a stereoelectronic interaction with O4′, which in turn counteracts the steric effect of the bulk and pushes the N ⇄ S pseudorotational equilibrium to the more N-type conformation in **3** (Table 3). These observations are consistent with the relative ^{15}N-NMR chemical shifts,[13] where the ^{15}N deshielding increases in the order pyrrole < imidazole < pyrazole, suggesting that the pyrazolo system fused with the π-electron-deficient pyrimidine is less π-electron excessive than the fused pyrrolo system.

In our set of three purine β-D-ribofuranosyl-*C*-nucleosides **1–3**, we have chosen pyrazolo[4,3-*d*]pyrimidines as the *C*-substituents in **1** or **2** as the optimal isosteric and isoelectronic *C*-aglycone analogs of the adenine or guanine base in β-D-ribofuranosyl-*N*-nucleosides, whereas the pyrrolo[3,2-*d*]pyrimidine moiety in 9-deazaadenosine (**3**) can be considered clearly as the undesirable alternative. $\Delta H°$ values[1,7a] of the pseudorotational equilibria of adenosine ($\Delta H°$ = −4.6 kJ/mol) and guanosine ($\Delta H°$ = −3.2 kJ/mol) are the net result of the following driving forces: (i) the gauche effects of 2′-OH and 3′-OH with O4′ and the effect of 4′-CH_2OH, which are exclusively accounted for in the $\Delta H°$ value of **9** (0.4 kJ/mol), (ii) the gauche effect of the O2′—C2′—C1′—N(purine) fragment ($\Delta H°$ = −6.3 kJ/mol), which is clearly accounted for in our previous studies with 2′-deoxynucleosides,[7a] (iii) the steric effect of adenine and guanine, which has been quantified in the present work by the average *C*-substituent effect (average $\Delta\Delta H°$ = −7.8 kJ/mol, Table 3) in **1** and **2**, and (iv) the anomeric effect in adenosine and guanosine. The above considerations have enabled us to calculate for the first time the magnitude of the O4′—C1′—N9 anomeric effect

(12) The work is now in progress in our laboratory to evaluate a set of bulky *C*-alkyl nucleosides for the determination of the reference point(s) of maximally pseudoequatorially oriented *C*-aglycone in order to quantitate the anomeric effect in both purine and pyrimidine type β-D-ribofuranosyl-*N*-nucleosides. Note that it is not clear to us at this point whether the steric effect of a single bulky *C*-alkyl nucleoside would be adequate as a reference point to characterize both the purine and pyrimidine β-D-ribofuranosyl-*N*-nucleosides.

(13) Newkome, G. R.; Paudler, W. W. *Contemporary Heterocyclic Chemistry, Synthesis, Reactions and Applications*; John Wiley & Sons: New York, 1982; p 15.

in the biologically ubiquitous adenosine (eq 1b) and guanosine (eq 1c) on the basis of eq 1a:

$$\text{anomeric effect} = \Delta H^\circ \text{ of adenosine or guanosine} - [\Delta H^\circ \text{ from (i)} + \Delta H^\circ \text{ from (ii)} + \Delta\Delta H^\circ \text{ from (iii)}] \quad (1a)$$

$$\text{anomeric effect of adenine (in kJ/mol)} = -4.6 - (0.4 - 6.3 - 7.8) = +9.1 \quad (1b)$$

$$\text{anomeric effect of guanine (in kJ/mol)} = -3.2 - (0.4 - 6.3 - 7.8) = +10.5 \quad (1c)$$

Conclusion

The present work along with our previous data on pyrimidine β-D-ribofuranosyl-*C*-nucleosides[1d] clearly shows for the first time that the N ⇄ S pseudorotational equilibria of the constituent sugar moiety is significantly influenced by the steric and stereoelectronic nature of the *C*-substituent in **1–8**: (i) For β-D-ribofuranosyl-purine-*C*-nucleosides, formycin A (**1**) and formycin B (**2**), the π-electron system in pyrazole moieties is highly delocalized owing to conjugation with the fused π-deficient pyrimidine ring and is therefore not available to interact with furanose-O4′ lone pairs. Thus the *C*-purine aglycones adopt a sterically dictated pseudoequatorial orientation, which is achieved in S-type sugar conformations in **1** and **2**. This results in large negative ΔH° values for their N ⇄ S pseudorotational equilibria (Table 3). The steric effect generated by 8-aza-9-deazapurines in β-D-ribofuranosyl-*C*-nucleosides **1** and **2** (≈ −7.8 kJ/mol) was estimated by the subtraction of their ΔH° values from ΔH° of 1-deoxy-β-D-ribofuranose (**9**). By comparing ΔH° values of **1** and **2** with those of the pseudorotational equilibria in adenosine and guanosine,[7a] we were also able to quantify the O4′—C1′—N9 anomeric effect of adenine and guanine bases in the corresponding adenosine and guanosine. (ii) For all other β-D-ribofuranosyl-*C*-nucleosides **3–8**, we have found that the differences in the actual orientation of the C1′-substituents (and therefore the differences in their ΔH° values, Table 3) result from the changes in the net result of the stereoelectronic and the inherent steric effect of the *C*-aglycone. It was therefore not possible to assess the anomeric effect in pyrimidine β-D-ribofuranosyl-*N*-nucleosides owing to the absence of an appropriate maximally pseudoequatorially oriented reference pyrimidine β-D-ribofuranosyl-*C*-nucleoside or a bulky *C*-alkylglycoside.[12]

Clearly, the most important use of this work is the reparametrization of the molecular mechanics force field parameters, which presently use only the generalized atom type for the modeling of nucleosides and their analogs without taking the constituent aromatic system into consideration. We believe this study should also be useful to understand how the local structure variation takes place in DNA and RNA depending upon the local nucleobase sequence. The further implication of this work is to understand why the catalytic self-cleavage in some RNAs (*e.g.* the hammerhead ribozyme) takes place in a sequence-specific manner.

Experimental Section

Vicinal proton–proton coupling constants ($^3J_{HH}$) were measured (Table 1) at 500 MHz in D_2O solution (≈20 mM) in 10 K steps in the ranges 278–358 K for **1–3** and 278–363 K for **4** (Table 1). The computer program PSEUROT (version 5.4)[9] was used to calculate the best fit of the five conformational parameters[2] (P and Ψ_m for both N and S pseudorotamers and the mole fraction of the N (X_N) or S (X_S) conformer) to the three experimental temperature-dependent coupling constants ($^3J_{1'2'}$, $^3J_{2'3'}$, and $^3J_{3'4'}$). The PSEUROT fitting processes were performed by constraining either Ψ_m of the N and S forms to an identical value (for **1–4**) or P_N and Ψ_N of the minor conformer during the optimization (for **1–3**) (see footnotes of Table 2). The quality of the fits has been assessed through the rms of the analyses (<0.2 Hz for all compounds) and the ΔJ_{max} values (<0.5 Hz, Table 2). The hyperspace of various geometries that are accessible with the experimental $^3J_{HH}$ for the N and S conformers of **1–4** according to our PSEUROT analyses is also reported in Table 2. The enthalpy (ΔH°) and entropy (ΔS°) contributions to the free energy (ΔG^{298} at 298 K) characterizing the N ⇄ S pseudorotational equilibria of **1–4** were determined by plotting $\ln(X_S/X_N)$ versus $1000/T$. The equations of the straight lines were calculated through a least-squares fitting process (see Figure 1 for typical van't Hoff plots and Table 3 for the energetics).

Acknowledgment. We thank the Swedish Board for Technical Development (NUTEK) and the Swedish Natural Science Research Council (NFR) for generous financial support, and Wallenbergstiftelsen, Forskningsrådsnämnden (FRN), and the University of Uppsala for funds for the purchase of a 500-MHz Bruker AMX NMR spectrometer.